

Supplementary Information for:

**A spatially dynamic network underlies the generation of  
inspiratory behaviors**

Nathan A Baertsch<sup>1</sup>, Liza J Severs<sup>1</sup>, Tatiana M Anderson<sup>1</sup>, and Jan-Marino Ramirez<sup>1,2</sup>

<sup>1</sup>Center for Integrative Brain Research; Seattle Children's Research Institute; Seattle,  
WA, USA

<sup>2</sup>Departments of Neurological Surgery and Pediatrics; University of Washington; Seattle,  
WA, USA

**Corresponding Author and Lead Contacts:**

Nathan Baertsch (nathan.baertsch@seattlechildrens.org) or Nino Ramirez  
(jan.ramirez@seattlechildrens.org)

**This PDF file includes:**

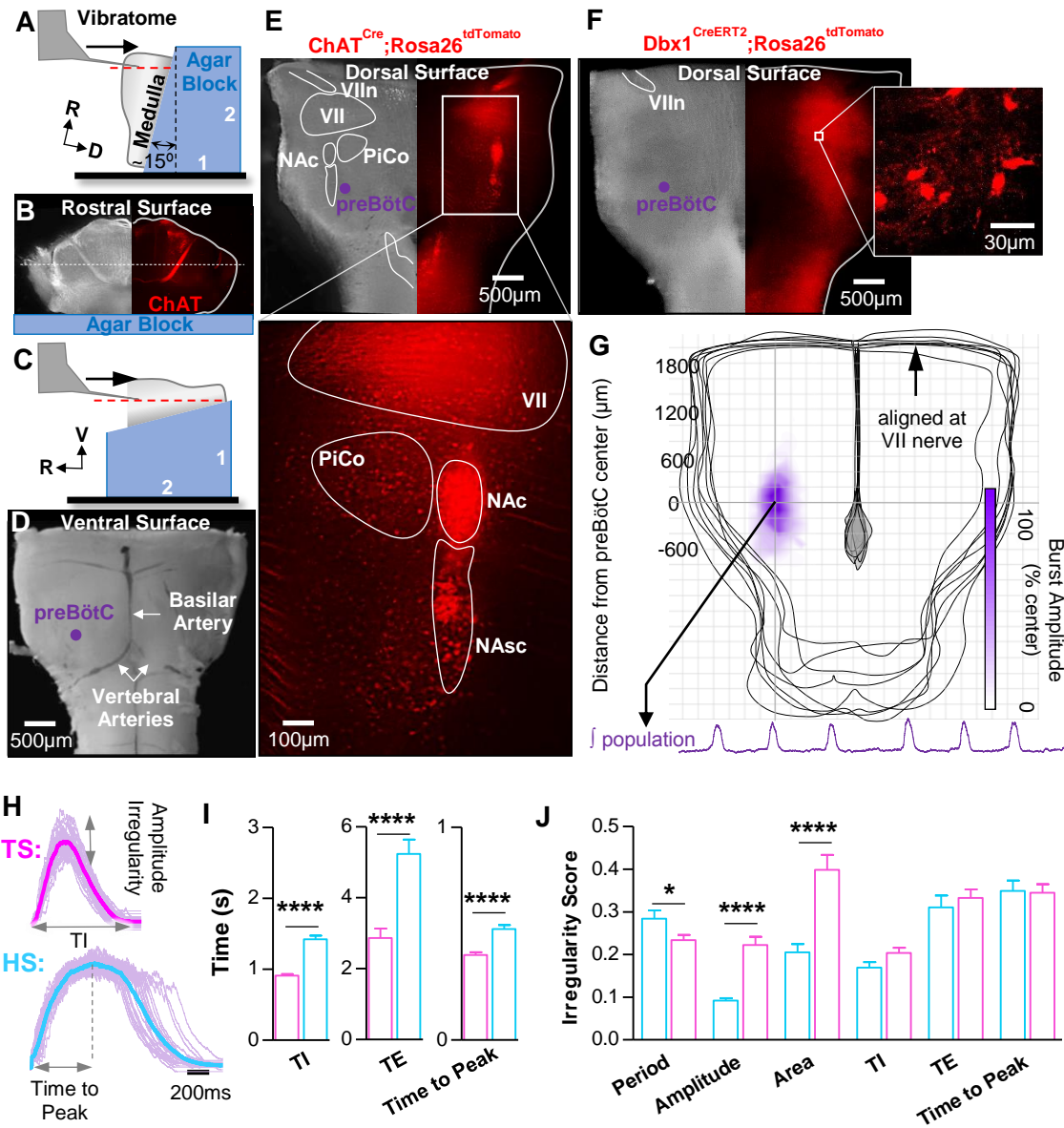
Figs. S1 to S5

Table S1

Supplementary text: detailed methods

References for SI reference citations

## Supplemental Figures:



**Fig S1:** Preparation of a horizontal medullary slice for characterization of the inspiratory column in-vitro. A) The medulla is sectioned from rostral to caudal in the transverse plane to B) expose the facial nerve (VIIIn) on the rostral surface (bright field, left; ChAT-tdTomato fluorescence, right). C) The medulla is then reoriented to make a single horizontal section ~850 $\mu$ m from the ventral surface. D) Anatomical landmarks on the ventral and E) dorsal surface of the horizontal slice showing the location of the preBötC (bright field, left; ChAT-tdTomato fluorescence, right). F) Dbx1-tdTomato fluorescence in the horizontal slice (insets are 20X images of Dbx1 neurons at the preBötC and rostral to the preBötC). G) Map of inspiratory spiking activity recorded by moving an extracellular electrode in 100 $\mu$ m steps across the horizontal slice. Heat map (purple) shows integrated burst amplitude. Trace shows example rhythmic activity recorded from the preBötC based on anatomical landmarks. VIIIn, facial nerve; VII, facial nucleus; NAc, compact division of the nucleus ambiguus; NAsc, semi-compact division of the nucleus ambiguus; PiCo, post-inspiratory complex. H) 20 overlaid bursts for transverse (TS) and horizontal (HS) slices depicting measured burst parameters. I) Group data from n=40 transverse and n=41 horizontal slices comparing burst parameters and J) irregularity scores. (\* $p > 0.05$ , \*\*\*\* $p > 0.0001$ ; means $\pm$ SEM)

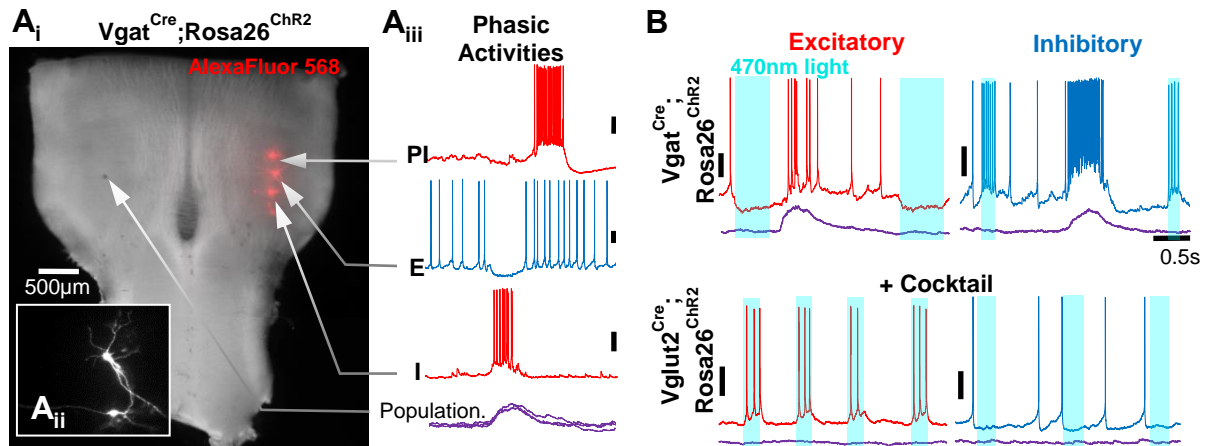


**Fig S2:** Spatial and functional characterization of respiratory neurons in the horizontal slice preparation. A) Example patch clamp recording experiment from a  $Vgat^{Cre};Rosa26^{ChR2}$  mouse. Patch pipettes containing AlexaFluor 568 were used to determine the location of each recorded neuron along the ventral medulla. Merged bright field and fluorescent images of the dorsal surface of the horizontal slice (Ai). Inset shows example 20X image of AlexaFluor 568 filled neurons (Aii). Inspiratory, expiratory, or post-inspiratory phasic activities of each neuron was determined relative to inspiratory population recording from the contralateral preBötC (grey) (Aiii). B) Representative optogenetic stimulations used to classify neurons as excitatory (red) or inhibitory (blue) in  $Vgat^{Cre};Rosa26^{ChR2}$  and  $Vglut2^{Cre};Rosa26^{ChR2}$  mice. Optogenetic stimulations in  $Vglut2^{Cre};Rosa26^{ChR2}$  were performed in the presence of a cocktail of synaptic blockers.

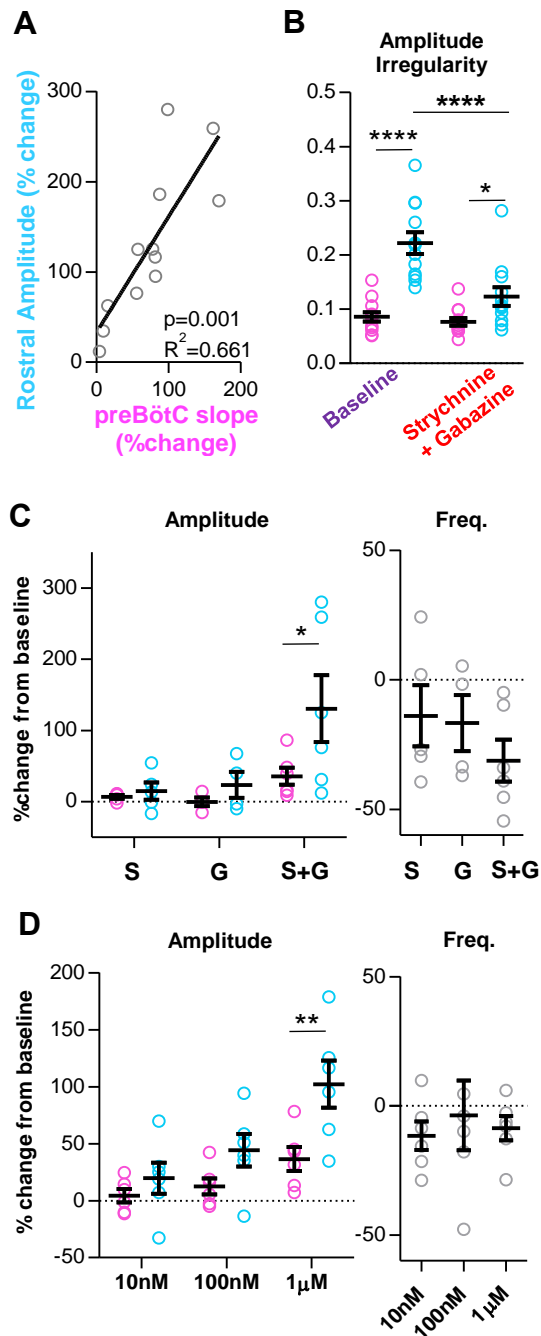


**Fig S3:** Spatial reconfiguration is regulated by the amount of network inhibition A) Changes in preBötC burst slope and rostral burst amplitude following suppression of inhibition shared a positive linear relationship. B) Burst amplitude irregularity scores at the preBötC center and in the rostral column at baseline and following suppression of inhibition. C) Changes in burst amplitude and frequency in horizontal slices following individual application of strychnine (S), gabazine (G), or both (S+G). D) Dose dependent changes in burst amplitude and frequency following co-application of strychnine and gabazine. (\* $p>0.05$ , \*\*\* $p>0.001$ ; means $\pm$ SEM)

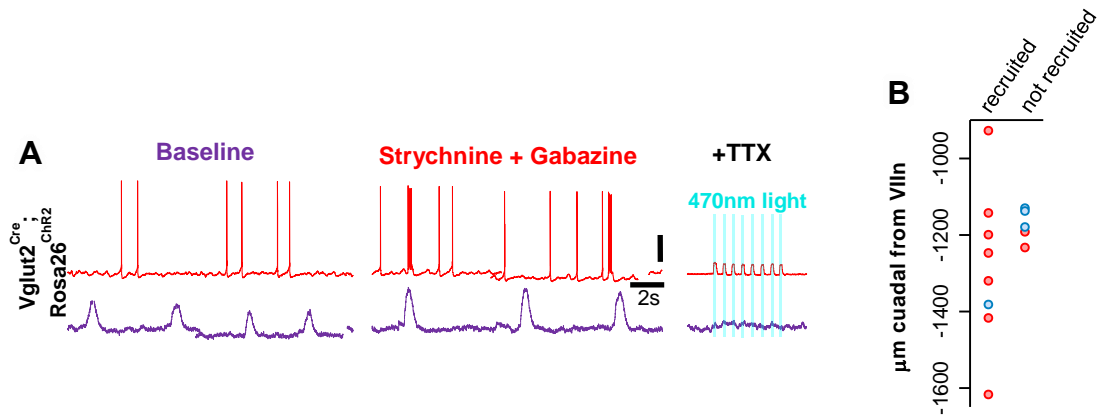


**Fig S4:** Inhibition restrains excitatory neurons in the rostral column from firing during inspiratory bursts. A) Representative intracellular (top) recording from a tonic spiking neuron in the rostral column and concurrent preBötC population activity (below) from a  $Vglut2^{Cre}; Rosa26^{ChR2}$  horizontal slice. The neuron was recruited to fire during inspiratory bursts following application of strychnine and gabazine ( $1\mu\text{M}$  each). Depolarizing responses to photo-stimulations in the presence of TTX ( $1\mu\text{M}$ ) indicate that this neuron is  $Vglut2^+$ . Vertical scale bar= $20\text{mV}$ . B) Quantified rostrocaudal locations relative to the VII nerve for neurons that were, and were not, recruited to fire during inspiratory bursts.

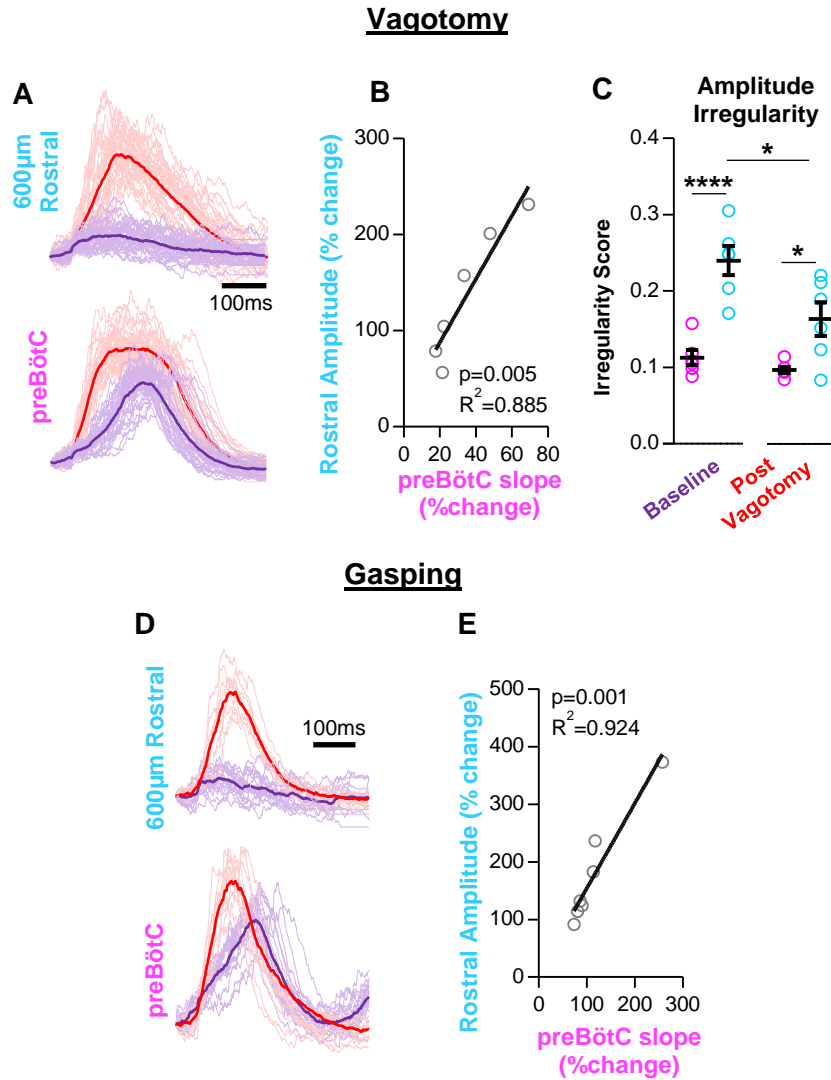


**Fig S5:** Inspiratory burst parameters following vagotomy and during hypoxia-induced gasping. A) Overlaid burst waveforms with average for 20 consecutive bursts in the rostral column and at the preBötC demonstrating changes in burst shape elicited by removal of vagal sensory feedback. B) Positive linear relationship between changes in preBötC burst slope and rostral burst amplitude elicited by vagotomy. C) Irregularity scores at the preBötC and  $558 \pm 20 \mu\text{m}$  rostral at baseline and following vagotomy. D) Overlaid burst waveforms with average for 10 bursts during eupnea (purple) and gasping (red). E) Positive linear relationship between change in preBötC burst rise slope and rostral burst amplitude.

**Table S1:** Statistical summary by figure panel.

<b><u>Figure</u></b>	<b><u>Test</u></b>	<b><u>Comparison</u></b>	<b><u>Values</u></b>	<b><u>N</u></b>
<b>1B</b>	two-tailed t-test with Welch's correction	Period: HS vs TS	p<0.0001; t=5.540	40 vs 41
<b>S1I</b>	two-tailed t-test with Welch's correction	TI: HS vs TS	p<0.0001; t=8.924	40 vs 41
	two-tailed t-test with Welch's correction	TE: HS vs TS	p<0.0001; t=4.919	40 vs 41
	two-tailed t-test with Welch's correction	Time to Peak: HS vs TS	p<0.0001; t=5.338	40 vs 41
	two-tailed t-test with Welch's correction	Period: HS vs TS	p=0.368; t=2.133	40 vs 41
<b>1C</b>	two-tailed t-test with Welch's correction	Amplitude: HS vs TS	p<0.0001; t=6.392	40 vs 41
	two-tailed t-test with Welch's correction	Area: HS vs TS	p<0.0001; t=4.801	40 vs 41
	two-tailed t-test	TI: HS vs TS	n.s.; p=0.0624; t=1.890	40 vs 41
<b>S1J</b>	two-tailed t-test with Welch's correction	TE: HS vs TS	n.s.; p=0.5190; t=0.6482	40 vs 41
	two-tailed t-test	Time to Peak: HS vs TS	n.s.; p=0.8792; t=0.1525	40 vs 41
	two-way RM ANOVA		Interaction: p= 0.0007; F=4.050	2 groups
<b>1E</b>	Bonferroni's multiple comparison tests	time=0.25: HS vs TS	n.s.; p>0.05; t=1.927	5 vs 4
		time=0.75: HS vs TS	p<0.001; t=4.655	5 vs 4
		time=1.25: HS vs TS	p<0.001; t=4.349	5 vs 4
		time=1.75: HS vs TS	n.s.; p>0.05; t=2.465	5 vs 4
		time=2.25: HS vs TS	n.s.; p>0.05; t=2.735	5 vs 4
		time=2.75: HS vs TS	n.s.; p>0.05; t=1.018	5 vs 4
		time=3.25: HS vs TS	n.s.; p>0.05; t=1.115	5 vs 4
		time=3.75: HS vs TS	n.s.; p>0.05; t=0.4718	5 vs 4
		time=4.25: HS vs TS	n.s.; p>0.05; t=0.0	5 vs 4
<b>2C</b>	one-way ANOVA		p=0.022; F=4.08	3 groups
	Bonferroni's multiple comparison tests	Inspiratory vs Expiratory	n.s.; p>0.05; t=0.027	47 vs 11
		Inspiratory vs Post-Inspiratory	p<0.05; t=2.830	47 vs 6
		Expiratory vs Post-Inspiratory	n.s.; p>0.05; t=2.399	11 vs 6
	two-tailed t-test	Inspiratory: Excitatory vs Inhibitory	n.s.; p=0.299; t=1.05	25 vs 22
	two-tailed t-test	Expiratory: Excitatory vs Inhibitory	n.s.; p=0.181; t=1.452	4 vs 7
	<b>3B</b>	two-tailed paired t-test	preBötC vs rostral	p=0.0007; t=4.618
<b>S3A</b>	linear regression	preBotC slope vs rostral amplitude	p=0.0013; R <sup>2</sup> =0.661	12 pairs
<b>S3B</b>	one-way RM ANOVA		p<0.0001; F=45.23	4 groups
	Bonferroni's multiple comparison tests	preBotC baseline vs rostral baseline	p<0.0001; t=9.732	12 pairs
		preBotC baseline vs preBotC inhibition block	n.s.; p>0.05; t=0.6643	12 pairs
		preBotC baseline vs rostral inhibition block	n.s.; p>0.05; t=2.668	12 pairs
		rostral baseline vs preBotC inhibition block	p<0.0001; t=10.4	12 pairs
		rostral baseline vs Rostral inhibition block	p<0.0001; t=7.065	12 pairs
		preBotC inhibition block vs rostral inhibition block	p<0.05; t=3.332	12 pairs
		two-way ANOVA		Interaction: p= 0.1847; F=1.814;
Bonferroni's multiple comparison tests	strychnine: preBötC vs rostral	n.s.; p>0.05; t=0.2249	5 vs 5	
	strychnine: preBötC vs rostral	n.s.; p>0.05; t=0.5956	4 vs 4	
	strychnine + gabazine: preBötC vs rostral	p<0.05; t=2.89	6 vs 6	
one-way ANOVA	Frequency	p=0.422; F=0.929	3 groups	
<b>S3D</b>	two-way RM ANOVA		Interaction: p= 0.0015, F=9.115	3 groups
	Bonferroni's multiple comparison tests	10nm: preBötC vs rostral	n.s.; p>0.05; t=0.8374	6 vs 6
		100nm: preBötC vs rostral	n.s.; p>0.05; t=1.724	6 vs 6

3C	one-way ANOVA	1 $\mu$ m: preBötC vs rostral	p<0.01; t=3.579	6 vs 6
	two-way ANOVA	Frequency	p=0.741; F=0.310	3 groups
S4B 4B	Bonferroni's multiple comparison tests	x=0, y=1100: control vs inhibition block	p=0.0001	8 vs 4
		x=0, y=1000: control vs inhibition block	p=0.0211	8 vs 4
		x=0, y=800: control vs inhibition block	p=0.0004	8 vs 4
		x=0, y=700: control vs inhibition block	p=0.0002	8 vs 4
		x=0, y=600: control vs inhibition block	p=0.0029	8 vs 4
		x=0, y=500: control vs inhibition block	p<0.0001	8 vs 4
		x=0, y=400: control vs inhibition block	p=0.0583	8 vs 4
		x=-100, y=600: control vs inhibition block	p=0.0114	8 vs 4
		x=-200, y=700: control vs inhibition block	p<0.0001	8 vs 4
		x=-200, y=600: control vs inhibition block	p=0.0029	8 vs 4
		x=-200, y=400: control vs inhibition block	p=0.0045	8 vs 4
		x=100, y=1200: control vs inhibition block	p=0.0178	8 vs 4
		x=100, y=900: control vs inhibition block	p=0.0004	8 vs 4
		x=100, y=700: control vs inhibition block	p=0.0101	8 vs 4
		x=100, y=600: control vs inhibition block	p=0.0331	8 vs 4
		x=200, y=800: control vs inhibition block	p=0.0090	8 vs 4
		x=200, y=700: control vs inhibition block	p=0.0111	8 vs 4
		x=200, y=600: control vs inhibition block	p=0.0304	8 vs 4
		x=200, y=500: control vs inhibition block	p=0.0093	8 vs 4
		x=200, y=400: control vs inhibition block	p=0.0246	8 vs 4
		x=300, y=500: control vs inhibition block	p=0.0004	8 vs 4
		x=300, y=400: control vs inhibition block	p=0.0058	8 vs 4
		x=300, y=300: control vs inhibition block	p=0.0006	8 vs 4
		x=300, y=200: control vs inhibition block	p=0.0116	8 vs 4
		x=300, y=0: control vs inhibition block	p=0.0039	8 vs 4
		all other x,y coordinates	n.s. p<0.05	8 vs 4
		two-tailed t-test with Welch's correction	recruited vs not recruited	p=0.197; t=1.428
	one-way ANOVA		p<0.0001; F=14.24	8 groups
	Bonferroni's multiple comparison tests	-1000 $\mu$ m vs -500 $\mu$ m	n.s.; p>0.05; t=2.58	6 vs 6
		-1000 $\mu$ m vs 0 $\mu$ m	p<0.01; t=3.897	6 vs 6
		-1000 $\mu$ m vs 500 $\mu$ m	p<0.05; t=3.492	6 vs 6
		-1000 $\mu$ m vs 1000 $\mu$ m	n.s.; p>0.05; t=1.654	6 vs 6
		-1000 $\mu$ m vs 1500 $\mu$ m	n.s.; p>0.05; t=1.089	6 vs 6
		-1000 $\mu$ m vs off slice	p<0.01; t=3.928	6 vs 6
		-500 $\mu$ m vs 0 $\mu$ m	n.s.; p>0.05; t=1.317	6 vs 6
		-500 $\mu$ m vs 500 $\mu$ m	n.s.; p>0.05; t=0.9123	6 vs 6
		-500 $\mu$ m vs 1000 $\mu$ m	n.s.; p>0.05; t=0.9257	6 vs 6
		-500 $\mu$ m vs 1500 $\mu$ m	n.s.; p>0.05; t=1.491	6 vs 6
		-500 $\mu$ m vs off slice	p<0.0001; t=6.508	6 vs 6
		0 $\mu$ m vs 500 $\mu$ m	n.s.; p>0.05; t=0.4046	6 vs 6
		0 $\mu$ m vs 1000 $\mu$ m	n.s.; p>0.05; t=2.243	6 vs 6
		0 $\mu$ m vs 1500 $\mu$ m	n.s.; p>0.05; t=2.808	6 vs 6
		0 $\mu$ m vs off slice	p<0.0001; t=7.825	6 vs 6
		500 $\mu$ m vs 1000 $\mu$ m	n.s.; p>0.05; t=1.838	6 vs 6
		500 $\mu$ m vs 1500 $\mu$ m	n.s.; p>0.05; t=2.403	6 vs 6
		500 $\mu$ m vs off slice	p<0.0001; t=7.421	6 vs 6



		1000µm vs 1500µm	n.s.; p>0.05; t=0.5654	6 vs 6
		1000µm vs off slice	p<0.0001; t=5.583	6 vs 6
		1500µm vs off slice	p<0.001; t=5.017	6 vs 6
<b>4F</b>	one-way ANOVA	ipsilateral stim	p<0.001; F=11.84	3 groups
	Bonferroni's multiple comparison tests	R1 vs R2	p<0.01; t=4.215	7 vs 7
		R1 vs C	p<0.01; t=4.215	7 vs 7
		R2 vs C	n.s.; p>0.05; t=0	7 vs 7
	one-way ANOVA	contralateral stim	p<0.0001; F=39.2	3 groups
	Bonferroni's multiple comparison tests	R1 vs R2	p<0.0001; t=8.46	7 vs 7
		R1 vs C	n.s.; p>0.05; t=1.97	7 vs 7
		R2 vs C	p<0.0001; t=6.49	7 vs 7
<b>4H</b>	two-tailed paired t-test	R2: spontaneous vs inhibition block	p=0.0133; t=3.00	9 pairs
	two-tailed paired t-test	C: spontaneous vs inhibition block	n.s.; p=0.345; t=1.00	9 pairs
<b>5C</b>	two-tailed paired t-test	preBötC vs rostral	p=0.0074; t=4.346	6 pairs
<b>S5B</b>	linear regression	preBotC slope vs rostral amplitude	p=0.0052; R <sup>2</sup> =0.8847	6 pairs
<b>S5C</b>	one-way RM ANOVA		p<0.0001; F=26.16	4 groups
	Bonferroni's multiple comparison tests	preBotC baseline vs rostral baseline	p<0.0001; t=7.146	6 pairs
		preBotC baseline vs preBotC post vagotomy	n.s.; p>0.05; t=0.8854	6 pairs
		preBotC baseline vs rostral post vagotomy	n.s.; p>0.05; t=2.862	6 pairs
		rostral baseline vs preBotC post vagotomy	p<0.0001; t=8.032	6 pairs
		rostral baseline vs rostral post vagotomy	p<0.01; t=4.825	6 pairs
		preBotC post vagotomy vs rostral post vagotomy	p<0.05; t=3.747	6 pairs
<b>5D</b>	two-way ANOVA		Interaction: p= 0.0073; F=1.607	2 groups
	Bonferroni's multiple comparison tests	x=0, y=1800: control vs vagotomized	p=0.0007	5 vs 7
		x=0, y=1500: control vs vagotomized	p=0.0037	5 vs 7
		x=0, y=1200: control vs vagotomized	p=0.0003	5 vs 7
		x=-150, y=1500: control vs vagotomized	p=0.0015	5 vs 7
		x=-150, y=1200: control vs vagotomized	p=0.0186	5 vs 7
		x=150, y=1200: control vs vagotomized	p=0.0019	5 vs 7
		all other x,y coordinates	n.s. p<0.05	5 vs 7
<b>6B</b>	two-tailed paired t-test	preBötC vs rostral	p=0.0051; t=4.306	7 pairs
<b>S5E</b>	linear regression	preBotC slope vs rostral amplitude	p=0.0006; R <sup>2</sup> =0.9239	7 pairs
<b>6E</b>	one-way ANOVA		p<0.0001; F=10.71	4 groups
	Bonferroni's multiple comparison tests	preBötC vs 200µm	n.s.; p>0.05; t=0.09296	21 vs 4
		preBötC vs 400µm	p<0.01; t=4.127	21 vs 8
		preBötC vs 600µm	p<0.001; t=4.553	21 vs 8
		200µm vs 400µm	p<0.05; t=2.883	4 vs 8
		200µm vs 600µm	p<0.05; t=3.172	4 vs 8
		400µm vs 600µm	n.s.; p>0.05; t=0.3542	8 vs 8

## DETAILED METHODS:

**Animals.** All experiments were performed on neonatal (p4-p12) and adult (p38-p416) male and female CD1 or C57-BI6 mice bred at Seattle Children's Research Institute. For optogenetic experiments, *Vglut2<sup>Cre</sup>* and *Vgat<sup>Cre</sup>*(1) homozygous breeder lines were obtained from Jackson Laboratories (Stock numbers 028863 and 016962, respectively). Heterozygous *Dbx1<sup>CreERT2</sup>* mice were donated by Dr. Del Negro (College of William and Mary, VA) and a homozygous breeder line was generated at SCRI. *Dbx1<sup>CreERT2</sup>* dams were plug checked and injected at E9.5 with tamoxifen (24mg/kg, i.p.) to target preBötC neurons(2). Cre mice were crossed with homozygous mice containing a floxed STOP channelrhodopsin2 fused to an EYFP (Ai32) reporter sequence. Some Cre mice were crossed with homozygous Cre-dependent tdTomato expressing reporter mice (Ai14) for improved visualization of cell bodies. All mice were group housed with access to food and water *ad libitum* in a temperature controlled (22±1°C) facility with a 12hr light/dark cycle.

**In-vitro medullary slice preparations.** Horizontal medullary slices containing the ventral respiratory column were prepared from postnatal day 4-12 mice. Whole brainstems were dissected in ice cold artificial cerebrospinal fluid (aCSF; in mM: 118 NaCl, 3.0 KCl, 25 NaHCO<sub>3</sub>, 1 NaH<sub>2</sub>PO<sub>4</sub>, 1.0 MgCl<sub>2</sub>, 1.5 CaCl<sub>2</sub>, 30 D-glucose) equilibrated with carbogen (95% O<sub>2</sub>, 5% CO<sub>2</sub>). aCSF had an osmolarity of 305–312mOSM and a pH of 7.40– 7.45 when equilibrated with gas mixtures containing 5% CO<sub>2</sub> at ambient pressure. The dorsal surface of the brainstem was secured with super glue to an agar block cut at a ~15° angle (rostral end facing up). Using a vibratome (Leica 1000S), the brainstem was sectioned in the transverse plane in 200µm steps until the VII nerves were visualized. To section the brainstem in the horizontal plane, the agar block was reoriented to position the ventral surface of the brainstem facing up with the rostral end towards the vibratome blade. The blade was leveled with the ventral edge of the brainstem and a single ~850µm step was taken to generate the horizontal slice (see SI Appendix Fig. S1A-D). The angle of the horizontal section through the tissue is determined by the angle at which the agar block was cut and is critical for a successful horizontal slice preparation. Too much angle, and the caudal aspect of the slice will be too thick; too little angle, and it will be too thin. The size and shape of the central canal is a suitable landmark with a partially open “teardrop” shaped central canal indicative of a properly prepared

horizontal slice (see SI Appendix Fig. S2Ai). The preBötC can then be located lateral to the rostral end of the teardrop and approximately  $\frac{1}{2}$  -  $\frac{3}{4}$  of the distance between the midline and the lateral edge of the slice.

Transverse brainstem slices were also prepared. Similar to horizontal slices, brainstems were isolated and glued to an agar block (dorsal surface to agar with the rostral end up) and serial 200 $\mu$ m sections were made until the VII nerves were visible. Consecutive 550 $\mu$ m slices were then taken through the inspiratory column to generate four isolated transverse slices, two rostral to the preBötC, one containing the preBötC (identified using anatomical landmarks such as the XII nucleus, inferior olive, and size of the fourth ventricle (3), and one caudal to the preBötC (see Fig. 5D).

Slices were placed in a recording chamber containing circulating aCSF (15ml/min) warmed to 30°C. The [K<sup>+</sup>] in the aCSF was then gradually raised from 3mM to 8mM over ~10min to boost neuronal excitability. Rhythmic extracellular neuronal population activity was recorded by positioning glass pipettes (<1M $\Omega$  tip resistance) filled with aCSF on the surface of the slice. Signals were amplified 10,000X, filtered (low pass, 300Hz; high pass, 5kHz), rectified, integrated, and digitized (Digidata 1550A, Axon Instruments). The activity of single neurons was recorded using the blind patch clamp approach. Recording electrodes were pulled from borosilicate glass (4-8M $\Omega$  tip resistance) using a P-97 Flaming/Brown micropipette puller (Sutter Instrument Co., Novato, CA) and filled with intracellular patch electrode solution containing (in mM): 140 potassium gluconate, 1 CaCl<sub>2</sub>, 10 EGTA, 2 MgCl<sub>2</sub>, 4 Na<sub>2</sub>ATP, and 10 Hepes (pH 7.2). To map the location of recorded neurons, patch pipettes were backfilled with intracellular patch solution containing 2mg/ml Alexa Fluor568 Hydrazide (ThermoFisher). Neuronal activity was recorded in whole-cell configuration with a multiclamp amplifier in current clamp mode (Molecular Devices, Sunnyvale, CA). Extracellular and intracellular signals were acquired in pCLAMP software (Molecular Devices, Sunnyvale, CA). Following in-vitro experiments, the position of the extracellular electrode(s) was marked mechanically and fresh, unfixed slices were imaged to determine the coordinates of intracellular and extracellular recording sites relative to rostral edge of the slice (VII nerve; Y direction) and the midline (X direction).

**Optogenetic and pharmacological manipulations.** A glass fiber optic (0.24NA) connected to a blue (470nm) high-powered LED was positioned above the preBötC contralateral to the extracellular electrode and ipsilateral to the intracellular electrode. A 100 $\mu$ m diameter fiber optic was used to map light-evoked responses along the

horizontal slice, and a fiber optic with a diameter of 200 $\mu$ m was used for all other optogenetic manipulations. Power was set  $\leq 1$ mW/mm<sup>2</sup>. To determine the probability of light-evoking inspiratory bursts, 200ms light pulses were TTL-triggered every 20s to stimulate Dbx1 neurons at defined sites along the inspiratory column ( $\geq 50$  trails/site). Trials were excluded from the analysis if the light pulse occurred during an ongoing spontaneous inspiratory burst. In transverse slice yoked stimulation experiments, light pulses were threshold triggered from integrated preBötC activity, such that light pulses corresponded with the frequency and duration of spontaneous preBötC bursts. During intracellular recordings, neurons were classified as excitatory or inhibitory using an optogenetic approach. In Vgat<sup>Cre</sup>;Rosa26<sup>ChR2-EYFP</sup> slices, neurons that depolarized during photostimulation were classified as inhibitory, while those that hyperpolarized or did not respond were presumed to be excitatory (see SI Appendix Fig. S2B). Because a depolarizing response to stimulation of excitatory neurons could be driven synaptically instead of from channelrhodopsin2 expression directly, in Vglut2<sup>Cre</sup>;Rosa26<sup>ChR2-EYFP</sup> and Dbx1<sup>CreERT2</sup>;Rosa26<sup>ChR2-EYFP</sup> slices, neurons were classified as excitatory or inhibitory based on the presence or absence of a depolarizing response to light, respectively, following pharmacological blockade of synaptic transmission with a cocktail of synaptic blockers (20 $\mu$ M CNQX, 20 $\mu$ M CPP, 1 $\mu$ M strychnine, 1 $\mu$ M gabazine) or TTX (1 $\mu$ M) (see SI Appendix Fig. S2B).

**In-vivo surgical preparation.** Adult mice were anesthetized with urethane (1.5mg/kg, i.p.) and placed supine on a custom surgical table. The trachea was exposed through a midline incision and cannulated caudal to the larynx with a curved (180 degree) tracheal tube (24G). Mice then spontaneously breathed 100% O<sub>2</sub> throughout the remainder of the surgery and experimental protocol (except during hypoxia). ECG leads were placed on the fore and hind paw to monitor heart rate. Core temperature was monitored and maintained with a heat lamp. Adequate depth of anesthesia was determined via heart rate and breathing frequency responses to toe pinch and adjusted if necessary with supplemental urethane (i.p.) prior to experimental protocols. The hypoglossal nerve (XII) was isolated unilaterally, cut distally and recorded from using a fire polished pulled glass pipette filled with aCSF connected to a suction electrode. Electrical activity from the brainstem and XII nerve was amplified (10,000X), filtered (low pass 300Hz, high pass 5kHz), rectified, integrated, and digitized (Digidata 1550A, Axon Instruments). The vagus nerve (X) was isolated bilaterally but left intact until a specific point in the experimental protocols. The trachea and esophagus were removed rostral to the tracheal tube, and the underlying muscles

were removed to expose the basal surface of the occipital bone. The portion of the occipital bone and dura overlying the ventral medullary surface were removed, and the exposed surface of the brainstem was superfused with warmed (~36°C) aCSF equilibrated with carbogen (95% O<sub>2</sub>, 5% CO<sub>2</sub>). To record neuronal population activity directly from the inspiratory column, tapered pulled glass pipettes with a sharp broken tip (<1MΩ tip resistance) filled with aCSF were advanced into the medulla ~200-500μm until integrated rhythmic activity reached a maximum. In some experiments, mice underwent either 1) a brief bout of anoxia (0% FiO<sub>2</sub>) to induce gasping, or 2) vagotomy to reduce sensory feedback inhibition.

**Microscopy.** Landmarks of the horizontal slice were characterized by imaging tdTomato fluorescence from whole horizontal slices generated from ChAT<sup>Cre</sup> and Dbx1<sup>CreERT2</sup> reporter mice. 2.5X images of the dorsal surface of horizontal slices were acquired on a Leica DM 4000 B epifluorescence microscope equipped with 405, 488, 548nm laser lines. 5X and 20X images were also acquired for inset images. All images were post-processed using Image-J software (Version 1.48). Following intracellular recording experiments, the location of each recorded neuron within the horizontal slice was immediately quantified by overlaying a 2.5X brightfield image and an epifluorescent image of Alexa Fluor 568 labelled cell(s).

**Statistical analysis.** Statistical analyses were performed using GraphPad Prism5 software and are summarized in SI Appendix Table S1. Groups were compared using appropriate two-tailed t-tests, or one-way or two-way ANOVAs with Bonferonni's multiple comparisons post hoc tests. Welch's correction was used for unequal variances. Linear regression analyses were used to determine relationships between breathing parameters. Differences were considered significant at p<0.05.

## References:

1. Vong L, *et al.* (2011) Leptin action on GABAergic neurons prevents obesity and reduces inhibitory tone to POMC neurons. *Neuron* 71(1):142-154.
2. Kottick A, Martin CA, & Del Negro CA (2017) Fate mapping neurons and glia derived from Dbx1-expressing progenitors in mouse preBotzinger complex. *Physiol Rep* 5(11).
3. Ruangkittisakul A, Kottick A, Picardo MC, Ballanyi K, & Del Negro CA (2014) Identification of the pre-Botzinger complex inspiratory center in calibrated "sandwich" slices from newborn mice with fluorescent Dbx1 interneurons. *Physiol Rep* 2(8).